Supplement of The Cryosphere, 19, 1725–1738, 2025
https://doi.org/10.5194/tc-19-1725-2025-supplement

The Cryosphere Open Access EGU

Supplement of

Speed-up, slowdown, and redirection of ice flow on neighbouring ice streams in the Pope, Smith, and Kohler region of West Antarctica

Heather L. Selley et al.

Correspondence to: Heather L. Selley (h.l.selley@leeds.ac.uk)

This file includes:

Figs. S1 to S4
Tables S1 to S2
Equation S1

Fig. S1.

Changes in flow direction and ice flux on Dotson and Crosson ice shelves. Panels **A-C** show **(A)** flow direction, **(B)** cumulative upstream ice flux and **(C)** flowlines in 2005. Panels **D-F** are the same for 2019. **(G)** Change in flow direction in 2019 compared to 2005. **(H)** Change in cumulative upstream ice flux in 2019 compared to 2005. Panels **(I)** and **(J)** show flow direction change and flow vectors in sub-regions near **(I)** the grounding line of Kohler East Glacier and **(J)** the division between Kohler West and Kohler East. The upstreamice flux in panels **(B)** and **(E)** are calculated along the flow lines shown in panels **(C)** and **(D),** respectively.

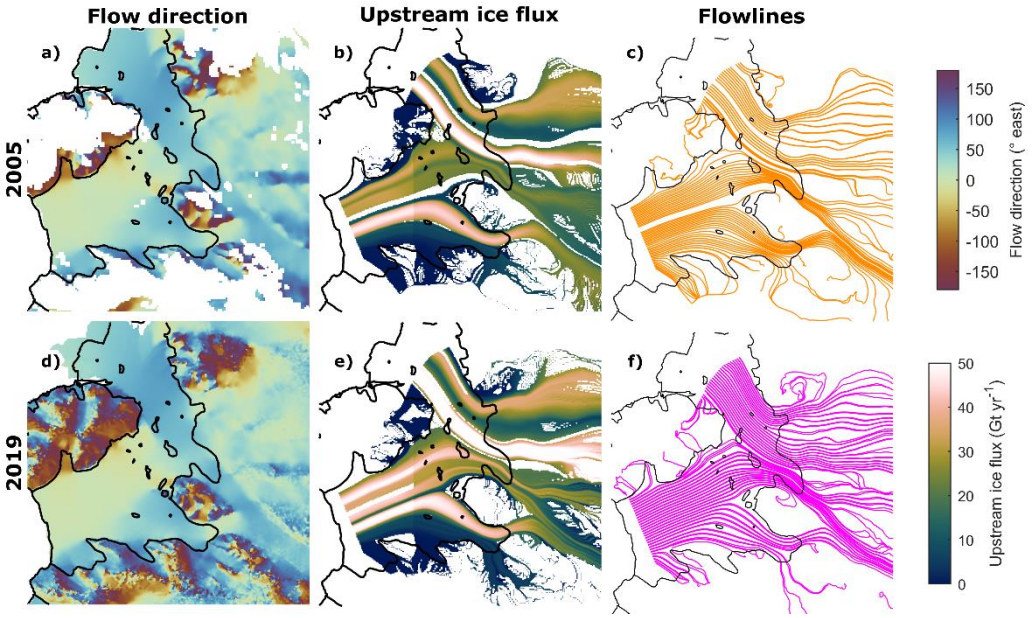

Fig. S2.

Observed ice speed of the Pope, Smith East, Smith West, Kohler glaciers (PSK) and Crosson Ice Shelf and the associated error estimate (right). Satellite observations included in each annual velocity map are

outlined in Table S1. The grounding line location (solid black line), the inland limit of the drainage basin (solid grey line) and the location of the 4 flow lines (dashed black lines) are also shown. The measurements are superimposed over Bedmachine bedrock topography (Morlighem et al., 2011). First shown are the Sentinel-1 ice speed maps 2015-2022 followed by the MeASUREs dataset 2005-2016.

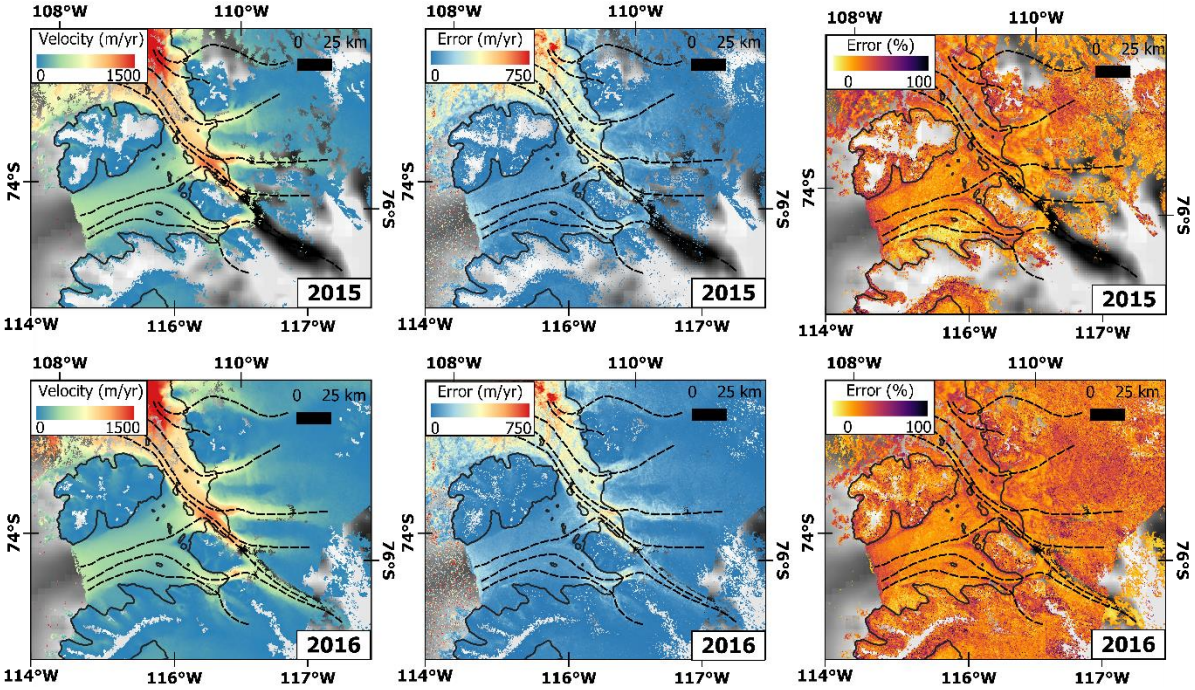

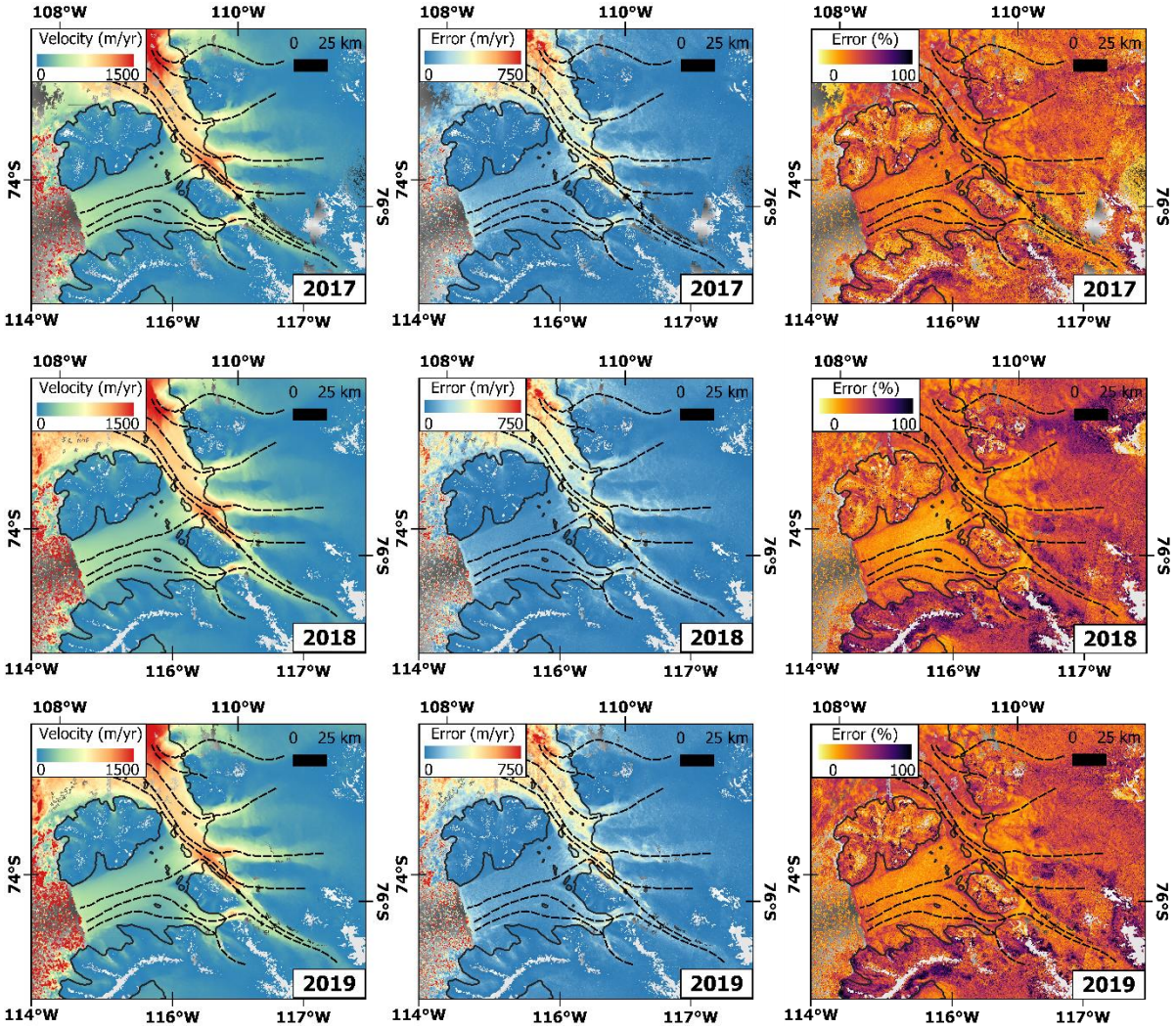
108°W
110°W
Velocity (m/yr)
0
1500
0 25 km
74°S
76°S
114°W
116°W
117°W
2017
Error (m/yr)
750
Error (%)
100
2018
2019

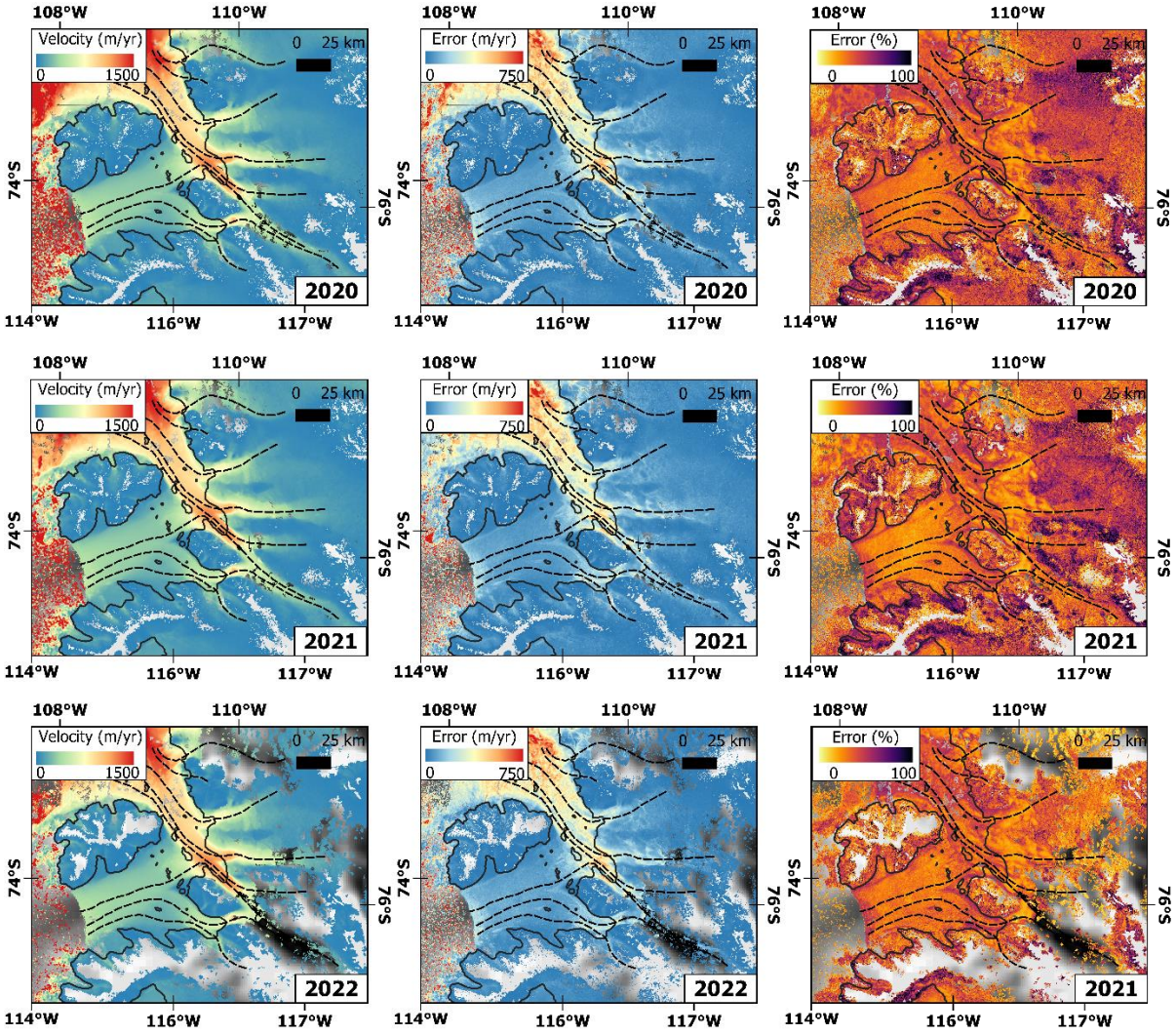
108°W
110°W
Velocity (m/yr)
0
1500
0 25 km
74°S
76°S
114°W
116°W
117°W
2020
Error (m/yr)
0
750
Error (%)
100
2021
2022

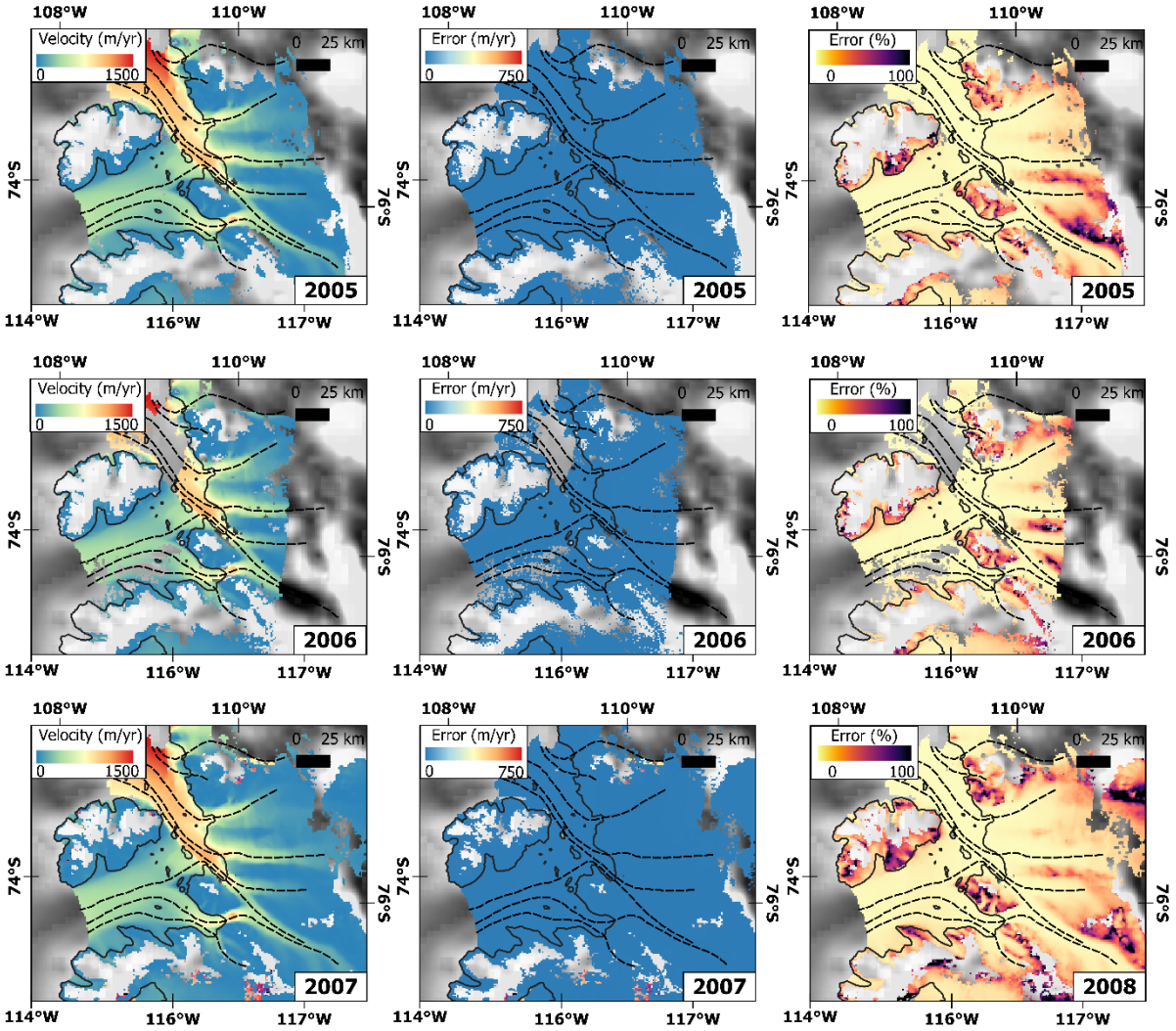
108°W
110°W
Velocity (m/yr)
0
1500
0
25 km
74°S
76°S
114°W
116°W
117°W
2005
Error (m/yr)
750
2005
Error (%)
100
2005
Velocity (m/yr)
2006
Error (m/yr)
2006
Error (%)
2006
Velocity (m/yr)
2007
Error (m/yr)
2007
Error (%)
2008

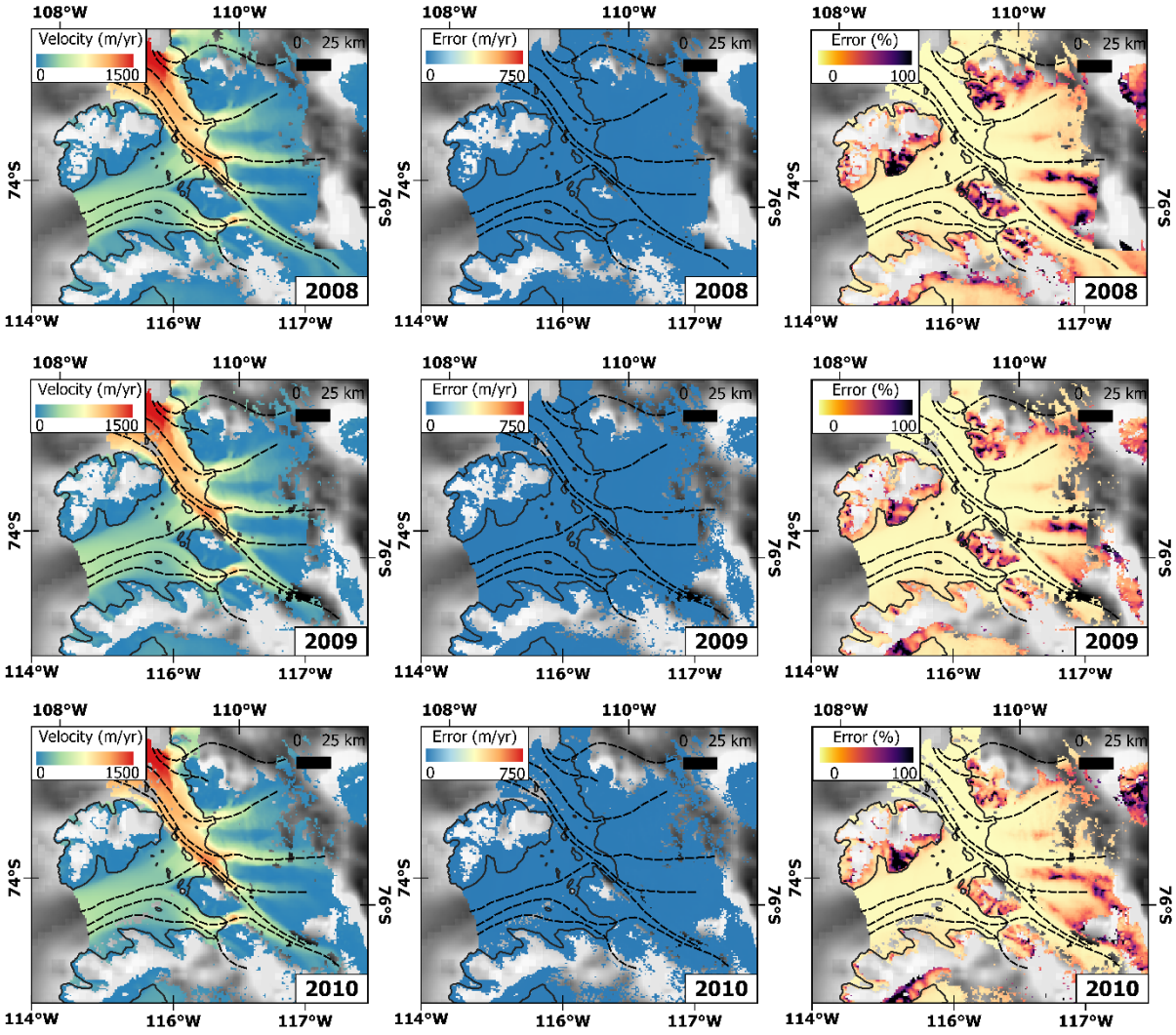
108°W
110°W
Velocity (m/yr)
0
1500
0 25 km
74°S
76°S
114°W
116°W
117°W
2008
Error (m/yr)
750
Error (%)
100
2009
2010

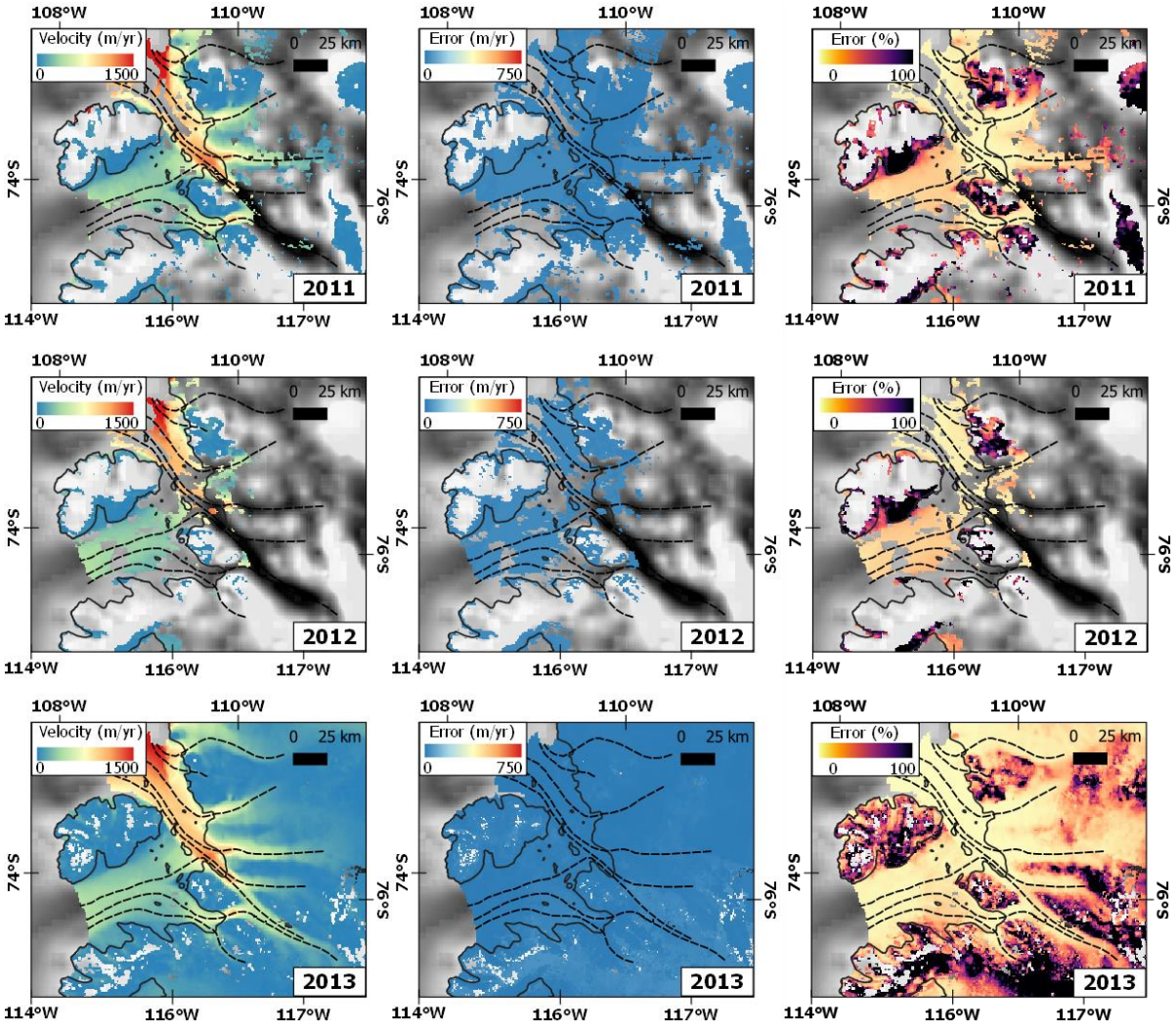
108°W
110°W
Velocity (m/yr)
0
1500
0 25 km
74°S
76°S
114°W
116°W
117°W
2011
Error (m/yr)
750
Error (%)
100
2012
2013

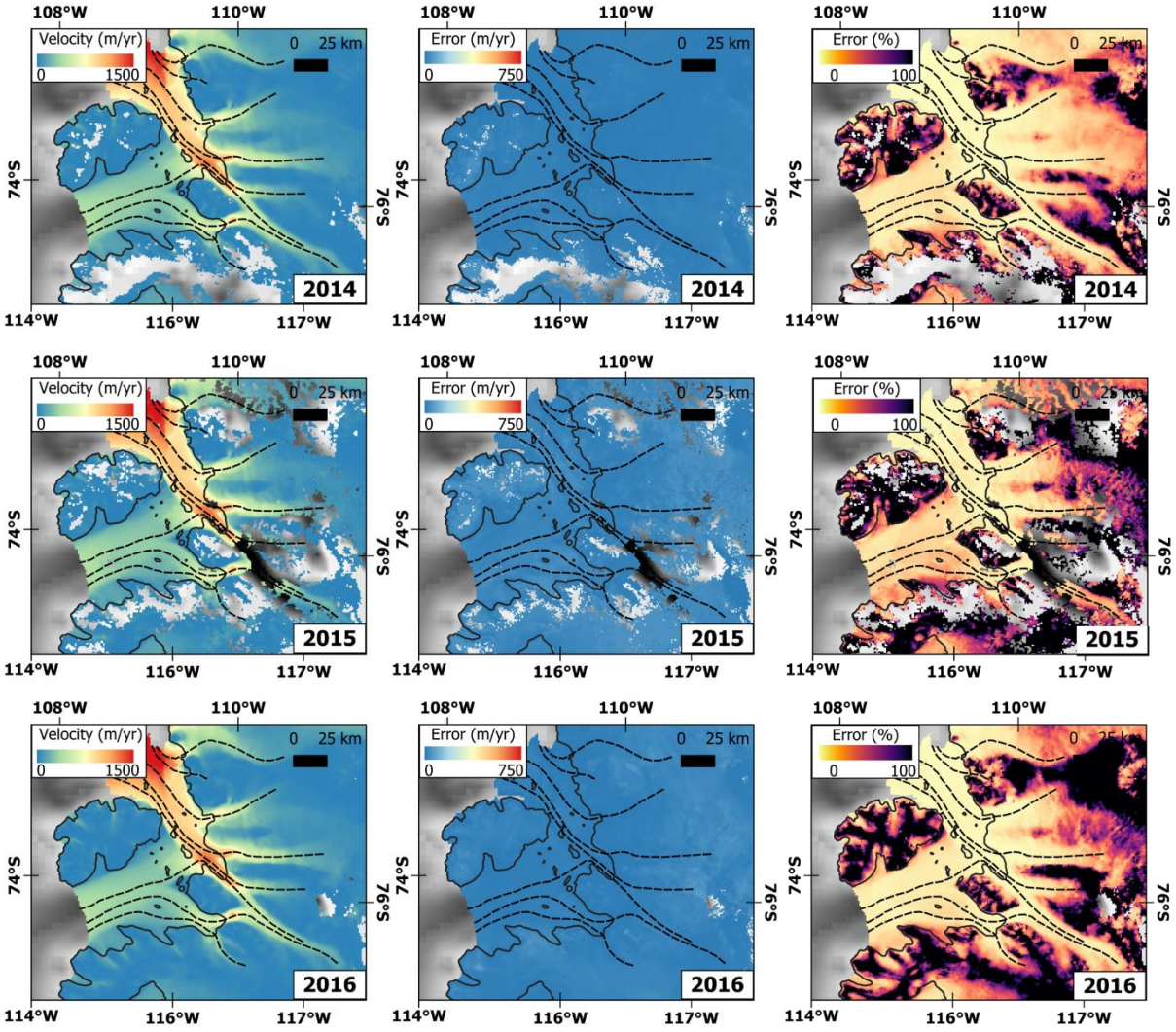
108°W
110°W
Velocity (m/yr)
0
1500
0 25 km
74°S
76°S
114°W
116°W
117°W
2014
Error (m/yr)
750
Error (%)
100
2015
2016

Fig. S3.
Observed area of damage behind the compressive arch on the Crosson Ice Shelf from MODIS imagery (black) and the distance to Bear Peninsula from the crack on the Crosson Ice Shelf (blue).

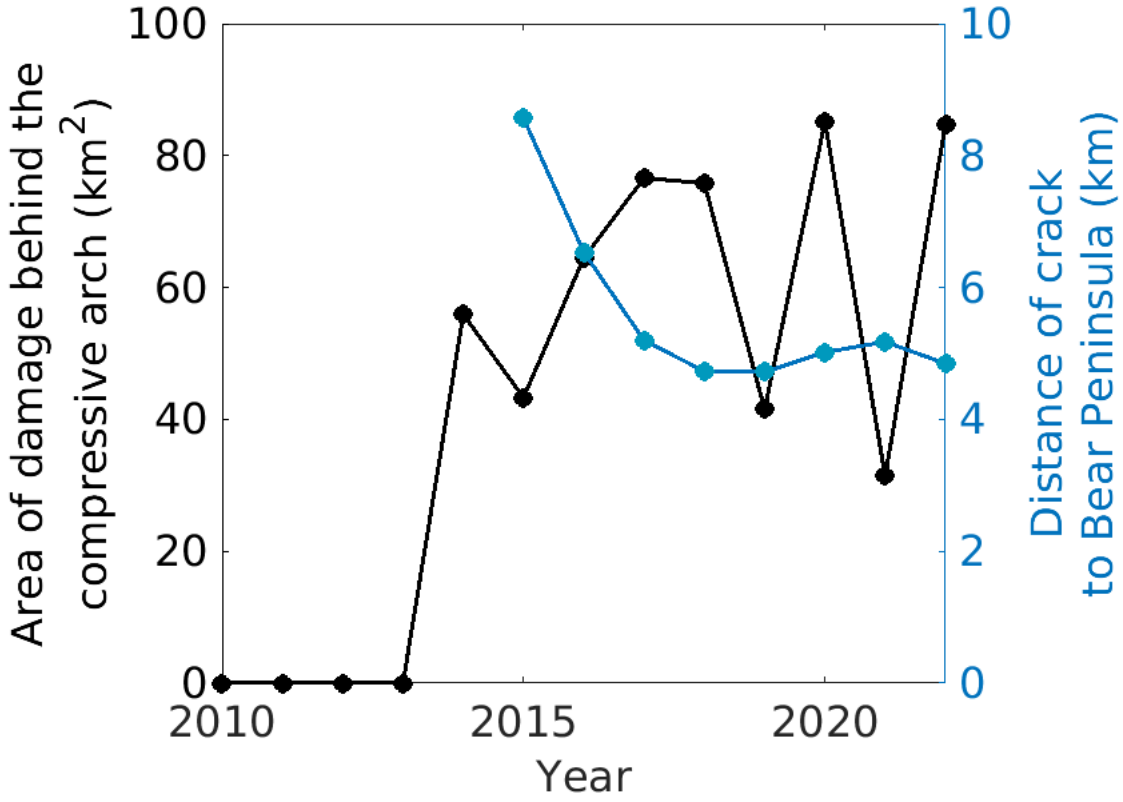

Table S1.
Summary of flow direction changes in the Regions of Interest (ROI) identified in Figure 4 based on ice speed and flow direction data (ROI1 referring to the region shown in Figure 4c and RO2 referring to the Figure 4d region. This clearly has been a progressive change in flow direction over time, particularly since 2009 at ROI2.

Time	ROI 1		ROI 2	
	Flow Direction (degrees east of north)	Error (degrees)	Flow Direction (degrees east of north)	Error (degrees)
'30-Dec-1996'	25.06	0.09	30.19	0.18
'30-Dec-2000'	26.45	0.26	23.90	0.69
'30-Dec-2005'	26.33	0.11	25.94	0.21
'30-Dec-2006'	26.42	0.21	25.54	0.45
'30-Dec-2007'	25.30	0.12	26.74	0.21
'30-Dec-2008'	25.39	0.16	25.51	0.32
'30-Dec-2009'	25.89	0.13	28.31	0.20
'30-Dec-2010'	25.70	0.11	30.73	0.19
'30-Dec-2011'	25.72	0.61	31.85	1.35
'30-Dec-2012'	23.39	0.83	32.47	1.78
'30-Dec-2013'	25.33	0.13	34.64	0.62
'30-Dec-2014'	24.80	0.23	34.60	0.67
'30-Dec-2015'	24.54	0.44	34.50	0.86
'30-Dec-2016'	24.04	0.16	35.01	0.36
'30-Dec-2017'	23.34	0.07	37.00	0.13
'30-Dec-2018'	23.10	0.07	37.82	0.13
'30-Dec-2019'	22.79	0.06	38.41	0.12

Table S2. Input satellite data used to measure ice speed from 2005.06.01 to 2022.12.31, for all 16 annual velocity maps.

Annual Velocity Map Name	Satellite	Data Type	Time Period Covered (YYYY.MM.DD)	
2005-2006	MEaSUREs data represent an average of the following satellite imagery: ALOS, ENVISAT, LANDSAT-8, RADARSAT-1, RADARSAT-2, Sentinel-1A, Sentinel-1B, TDX and TSX	SAR and Optical	2005.06.01	2006.05.30
2006-2007			2006.06.01	2007.05.30
2007-2008			2007.06.01	2008.05.30
2008-2009			2008.06.01	2009.05.30
2009-2010			2009.06.01	2010.05.30
2010-2011			2010.06.01	2011.05.30
2011-2012			2011.06.01	2012.05.30
2012-2013			2012.06.01	2013.05.30
2013-2014			2013.06.01	2014.05.30
2014-2015			2014.06.01	2015.05.30
2015-2016			2015.06.01	2016.05.30
2016-2017			2016.06.01	2017.05.30
S1–2015	Sentinel-1A and Sentinel-1B	SAR	2015.01.01	2015.12.31
S1-2016			2016.01.01	2016.12.31
S1-2017			2017.01.01	2017.12.31
S1-2018			2018.01.01	2018.12.31
S1 -2019			2019.01.01	2019.12.31
S1-2020			2020.01.01	2020.12.31
S1-2021			2021.01.01	2021.12.31
S1-2022			2022.01.01	2022.12.31

Comparison of the Sentinel-1 and MeASUREs ice speed data overlap period between 2016 and 2017

We compared the two ice speed datasets in this time period in the 2.5 km diameter regions at the grounding line of all 8 glaciers (Table S3). Overall, the Sentinel-1 velocity measurements are slightly faster than MeASUREs result on all glaciers, with an average speed difference of 21 m/yr (5%) in 2016 and 17 m/yr (3 %) in 2017. If we remove the slower flowing Horrall and Vane glaciers which flow at 401 and 203 m/yr respectively, the absolute difference reduces slightly (19 and 13 m/yr respectively), but the percentage difference reduces substantially to 2 and 1 % for 2016 and 2017 respectively. This is well within the error on our speed measurements.

The majority of this speed difference is likely caused by differences in the underlying spatial resolution of the satellite data and the step and window size used for the feature tracking. It is well known (Lemos et al., 2018) that finer spatial resolution satellite datasets allow you to track ice speeds at high spatial resolution which then detect small regions of fast flow. Equally using a larger window and step size in the feature tracking step will tend to effectively smooth the output ice speed result which subtly reduces the average mean speed, and it also tends to increase spatial coverage slightly. As we move into an era with more SAR satellites that enable us to track ice speed at different resolution from different sensors for any one location, it will be increasingly important to characterise these differences, in the same way the satellite altimetry community is already doing for laser and multi-frequency radar altimetry products.

There is also a slight difference in the time periods covered by the two products: Sentinel runs Jan-Dec whereas MeASUREs runs from July to June. These differences may be due to error in the products; however, they may also be due to real geophysical change that occurs between the time periods. We used a linear fit in all ice speed trend analyses to minimise the impact of any offset between the two speed products.

Table S3. Comparison of the Sentinel-1 and MeASUREs ice speed data overlap period between 2016 and 2017

Time Period	Horrall	Kohler West	Kohler East	Smith West	Smith East	Pope	Vane	Haynes	Average (all)	Average (fast flowing)
MeASUREs minus S1 (m/yr)										
2016	-17	-18	-28	-8	-28	-14	-42	-15	-21	-19
2017	-33	-3	-28	-12	-6	-2	-21	-29	-17	-13
Average S1 Speed (m/yr)										
2022	401	715	1215	1188	1093	772	203	810	800	966
Difference between Measures and S1 speeds as % of 2022 speed										
2016	-4	-3	-2	-1	-3	-2	-20	-2	-5	-2
2017	-8	0	-2	-1	-1	0	-10	-4	-3	-1

Equation S1: Equation used to calculate deformation with the initial ice thickness and surface slope, then calculated it again with the new thickness and surface slope.

$$U = \left(2 * A/(n+1)\right) * (\rho_i * g * \ \alpha * H)^n * H$$

H = ice thickness

A = rate factor for ice (9.3e-25 $s^{-1}Pa^{-3}$)

n = flow law exponent (3)

ρ_i = ice density (917 kg/m^3)

g = acceleration due to gravity (9.81 m/s/s)

α = sine of the surface slope

References

Lemos, A., Shepherd, A., McMillan, M., Hogg, A. E., Hatton, E., and Joughin, I.: Ice velocity of Jakobshavn Isbræ, Petermann Glacier, Nioghalvfjerdsfjorden, and Zachariæ Isstrøm, 2015-2017, from Sentinel 1-a/b SAR imagery, Cryosphere, 12, 2087–2097, https://doi.org/10.5194/tc-12-2087-2018, 2018.

Morlighem, M., Williams, C. N., Rignot, E., An, L., Arndt, J. E., Bamber, J. L., Catania, G., Chauché, N., Dowdeswell, J. A., Dorschel, B., Fenty, I., Hogan, K., Howat, I., Hubbard, A., Jakobsson, M., Jordan, T. M., Kjeldsen, K. K., Millan, R., Mayer, L., Mouginot, J., Noël, B. P. Y., O'Cofaigh, C., Palmer, S., Rysgaard, S., Seroussi, H., Siegert, M. J., Slabon, P., Straneo, F., van den Broeke, M. R., Weinrebe, W., Wood, M., and Zinglersen, K. B.: BedMachine v3: Complete Bed Topography and Ocean Bathymetry Mapping of Greenland From Multibeam Echo Sounding Combined With Mass Conservation, Geophys Res Lett, 44, 11,051-11,061, https://doi.org/10.1002/2017GL074954, 2017.

Mouginot, J., Rignot, E., and Scheuchl, B.: Continent-Wide, Interferometric SAR Phase, Mapping of Antarctic Ice Velocity, Geophys Res Lett, 46, 9710–9718, https://doi.org/10.1029/2019GL083826, 2019.